Structure and Electrochemistry of Various Diruthenium(II,III) Tetrametallocenecarboxylates

Michael W. Cooke,[†] T. Stanley Cameron,[‡] Katherine N. Robertson,[‡] Jannie C. Swarts,[§] and Manuel A. S. Aquino*,[†]

Departments of Chemistry, St. Francis Xavier University, P.O. Box 5000, Antigonish, Nova Scotia, B2G 2W5, Canada, Dalhousie University, Halifax, Nova Scotia, B3H 4J3, Canada, and The University of the Free State, Bloemfontein, 9300, South Africa

Received September 4, 2002

A series of mixed-valent diruthenium(II,III) tetrametallocenecarboxylates of the form $Ru_2(\mu\text{-}O_2C(X)C_5H_4MCp)_4Cl$, where M = Fe(II) and X = nothing (**1**), $-CH_2-$ (**2**), $-CH_2CH_2-$ (**3**), $-CH{=}CH-$ (**5**), M = Ru(II) and X = nothing (**6**), and the corresponding dechlorinated alcohol di-adducts $[Ru_2(\mu\text{-}O_2C(X)C_5H_4MCp)_4(ROH)_2](PF_6)$, where M = Fe(II), R = ethyl or 1-propyl, and X = nothing (**7**), $-CH_2-$ (**8**), $-CH_2CH_2-$ (**9**), and $-CH{=}CH-$ (**10**), and M = Ru(II) and X = nothing (**11**), were synthesized and characterized. In addition, the partially substituted complex with the tentative formula $Ru_2(\mu\text{-}O_2CCH_3)_3(\mu\text{-}O_2C(X)C_5H_4FeCp)_4Cl$, where X = $-CH_2CH_2CH_2-$ (**4**), was partially characterized. Complex **7** was structurally characterized previously, and the structures of complexes **10** and **11** are reported here. The complexes differ significantly in the orientation of the metallocenyl rings with respect to each other. An extension of the electrochemical studies that previously revealed evidence of ferrocenyl−ferrocenyl communication in complex **7** shows that this interaction is absent as the X group is lengthened and saturated, but a small degree of communication is still present in complex **10**, which contains an unsaturated, conjugated, spacer. The trend in the ferrocenyl-based redox process for complexes **7**−**10** mimics that of the corresponding free acids. No interactions are seen in the ruthenocenyl derivative (**11**) due to the irreversibility of its ruthenocenyl-centered redox processes.

Introduction

The binding of metallocene(mono)carboxylates to transition metals[1] has received relatively little attention in the literature, and the only examples for which structural information is available, that we have encountered, involve ferrocenecarboxylic acids. These carboxylates can, of course, bind in ways such as any other carboxylates, and examples include η^1-unidentate binding to Cu(II)[2−4] and V(IV);[5] η^2-bidentate binding to Cu(II)[3,4] and Ru(II);[6] and μ^2,η^2-bridging to Ti(IV),[7] Cu(II),[8−10] Os(0),[11] and Mo(II).[12] An interesting example containing three different binding modes in one compound is the cluster compound $Na_2Mo_6Cl_8(O_2CC_5H_4FeCp)_6$, in which the ferrocenecarboxylate binds in an unidentate fashion to Mo(II), in a bridging fashion to both Mo(II) and Na(I) and in a tridentate fashion with one oxygen bound to an Mo(II) and the second oxygen bridging two sodium ions.[13]

In addition to the monocarboxylates mentioned there has been increased interest in 1,1′-ferrocenedicarboxylate and its use as a linker in the construction of small and extended arrays. Examples of these include a polymeric chain linking Fe^{III}cyclam units,[14] the bridging of two Zn(II) ions to form a large square,[15] and the linking of two osmium trimers.[11] Cotton and co-workers have recently used 1,1′-ferrocenecarboxylate to create dimers and squares involving quadruply bonded Mo_2^{4+} units as termini or vertexes.[16−18]

* To whom correspondence should be addressed. E-mail: maquino@stfx.ca.
[†] St. Francis Xavier University.
[‡] Dalhousie University.
[§] University of the Free State.

(1) There are examples of ferrocenecarboxylates bound to main group elements such as Sn, Ga, and Si; however, we will restrict our attention here to transition metals.

(2) Abuhijleh, A. L.; Woods, C. *J. Chem. Soc., Dalton Trans.* **1992**, 1249.
(3) Abuhijleh, A. L.; Politte, J.; Woods, C. *Inorg. Chim. Acta* **1994**, *215*, 131.
(4) Costa, R.; López, C.; Molins, E.; Espinosa, E.; Pérez, J. *J. Chem. Soc., Dalton Trans.* **2001**, 2833.
(5) Collison, D.; Mabbs, F. E.; Turner, S. S.; Powell, A. K.; McInnes, E. J. L.; Yellowlees, L. J. *J. Chem. Soc., Dalton Trans.* **1997**, 1201.
(6) Matas, L.; Moldes, I.; Soler, J.; Ros, J.; Alvarez-Larena, A.; Piniella, J. F. *Organometallics* **1998**, *17*, 4551.
(7) Bailey, A.; Shang, M.; Fehlner, T. P. *Inorg. Chem.* **2000**, *39*, 4374.
(8) Churchill, M. R.; Li, Y. J.; Nalewajek, D.; Schaber, P. M.; Dorfman, J. *Inorg. Chem.* **1985**, *24*, 2684.
(9) Costa, R.; López, C.; Molins, E.; Espinosa, E. *Inorg. Chem.* **1998**, *37*, 5686.
(10) López, C.; Costa, R.; Illas, F.; Molins, E.; Espinosa, E. *Inorg. Chem.* **2000**, *39*, 4560.
(11) Lee, S. M.; Cheung, K. K.; Wong, W. T. *J. Organomet. Chem.* **1996**, *506*, 77.
(12) Cotton, F. A.; Falvello, L. R.; Reid, Jr., A. H.; Tocher, J. H. *J. Organomet. Chem.* **1987**, *319*, 87.
(13) Prokopuk, N.; Shriver, D. F. *Inorg. Chem.* **1997**, *36*, 5609.
(14) Christie, S. D.; Subramanian, S.; Thompson, L. K.; Zaworotko, M. J. *J. Chem. Soc., Chem. Commun.* **1994**, 2563.
(15) Zevaco, T. A.; Gorls, H.; Dinjus, E. *Polyhedron* **1998**, *17*, 613.
(16) Cotton, F. A.; Daniels, L. M.; Lin, C.; Murillo, C. A. *J. Am. Chem. Soc.* **1999**, *121*, 4538.
(17) Cotton, F. A.; Lin, C.; Murillo, C. A. *Inorg. Chem.* **2001**, *40*, 478.

10.1021/om020729b CCC: $22.00
Publication on Web 11/23/2002

Chart 1

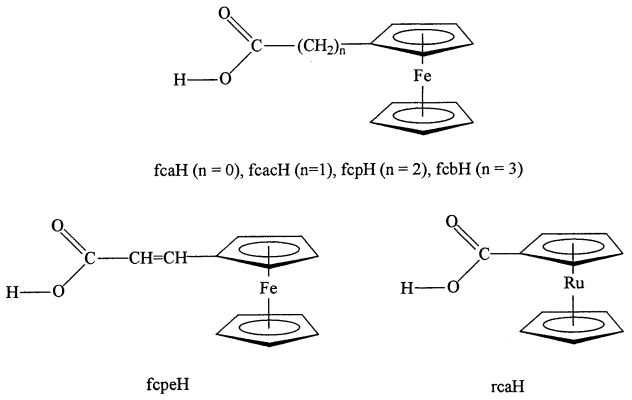

In a preliminary paper we recently reported on the structure and electrochemistry of the mixed-valent $[Ru_2(\mu\text{-}O_2CC_5H_4FeC_5H_5)_4(1\text{-propanol})_2](PF_6)$ complex (abbreviated as $[Ru_2(\mu\text{-fca})_4(1\text{-prop})_2](PF_6)$ where fca = ferrocenecarboxylate).[19] While the structure reflects the typical paddle-wheel geometry, similar to Churchill's dicopper(II,II)[8] and Cotton's dimolybdenum(II,II) analogue,[12] the electrochemistry revealed a small but significant interaction (electronic coupling) between the iron centers. Although we were not able to isolate it, there was clear evidence for a "multiple mixed-valent" intermediate with Fe^{III} and Fe^{II} centers (weakly coupled) and the strongly coupled Ru_2(III,II) core.[20]

This paper presents a full report on the synthetic, structural, electrochemical, and spectroscopic properties of a series of diruthenium(II,III) ferrocenecarboxylates (see Chart 1 for ligands and abbreviations), with both saturated and unsaturated chains linking the Cp ring and the μ^2-bridging carboxylate, COO^-, moiety. We also report the first structural example of a ruthenocenecarboxylate bound to a metal center in the complex $[Ru_2(\mu\text{-rca})_4(1\text{-propanol})_2](PF_6)$.

Experimental Section

Materials. All reagents were obtained from commercial suppliers and used as received, unless otherwise noted. Dichloromethane and 1,2-dichloroethane were distilled over CaH_2 under nitrogen. *N*,*N*-Dimethylformamide was dried over $MgSO_4$ and distilled under reduced pressure. Ferrocenecarboxylic (ferrocenoic) acid (fcaH) and ferrocenylacetic acid (fcacH) were supplied by Aldrich or prepared by the method of Reeves.[21] 3-Ferrocenylpropanoic acid (fcpH),[22] 4-ferrocenylbutanoic acid (fcbH),[23] and 3-ferrocenyl-2-propenoic acid (fcpeH)[22] were prepared by literature methods. Ruthenocenecarboxylic acid (rcaH) was prepared following the 2-chlorobenzoyl chloride route as described by Reeves[21] for the synthesis of ferrocenoic acid but by replacing ferrocene with ruthenocene. The resulting ruthenocenoic acid was characterized and found to be identical to an authentic sample prepared from lithiated ruthenocene via the method of Rausch.[24] $Ru_2(\mu\text{-}O_2CCH_3)_4Cl$ was prepared by the method of Mitchell et al.[25] and $[Ru_2(\mu\text{-}O_2CCH_3)_4(H_2O)_2](PF_6)$ using the procedure of Drysdale et al.[26]

Physical Measurements. Infrared spectra were recorded on a Bio-Rad FTS-175 spectrophotometer as KBr disks. Ultraviolet−visible spectra were obtained with a Varian 100 or a Varian 2300 spectrophotometer using matched 1 cm Hellma quartz cells. Effective magnetic moments were determined at room temperature using a Johnson Matthey MSB-1 magnetic susceptibility balance with $HgCo(SCN)_4$ as a calibrant ($\chi_g = 16.17 \times 10^{-6}$ cgs).[27] Cyclic voltammetry and Osteryoung square wave voltammetry (OSWV) were performed in 1,2-dichloroethane, dichloromethane, or *N*,*N*′-dimethylformamide using a BAS CV-50W voltammetric analyzer. The cell system consisted of a platinum button working electrode, a platinum wire auxiliary electrode, and a Ag/AgCl reference electrode or Ag wire pseudoreference. The ferrocenium/ferrocene couple was used as an internal reference and found to have an $E_{1/2} = 410$ mV vs Ag/AgCl ($\Delta E = 65$ mV) and $E_{1/2} = 86$ mV vs Ag wire ($\Delta E = 80$ mV). Measurements were normally performed on a 2 mM solution of the complex with 0.100 M tetrabutylammonium hexafluorophosphate, $[CH_3(CH_2)_3]_4NPF_6$ (TBAH), as the supporting electrolyte. All solutions were purged with argon for 15 min prior to each scan. Elemental analyses were performed by Canadian Microanalytical Service Ltd., Delta, B.C., Canada. X-ray data were collected and the structures solved at the DalX X-ray facility, Dalhousie University, Halifax, N.S., Canada.

$Ru_2(\mu\text{-fca})_4Cl$ (1). $Ru_2(\mu\text{-}O_2CCH_3)_4Cl$ (0.100 g, 0.21 mmol) was dissolved in 30 mL of hot methanol and concentrated to 20 mL. Ferrocenecarboxylic acid (fcaH) (0.291 g, 1.26 mmol) was dissolved separately in 30 mL of hot methanol and then combined with the above solution. The mixture was then refluxed for 6 h under argon and cooled at 4 °C overnight. The red-brown microcrystalline product was filtered, washed with 50 mL of methanol, and dried in vacuo. Yield = 0.148 g (60%). Mp = 220−222 °C (dec). Crystals suitable for X-ray diffraction could be grown by slow evaporation from 1,1,2,2-tetrachloroethane; however, crystal degradation in the X-ray beam, even at low temperatures, gave a structure that refined poorly (see later). Anal. Calcd (%) for $Ru_2Fe_4C_{44}H_{36}O_8Cl{\cdot}CH_3OH$: C, 45.58; H, 3.40; Cl, 2.99; Fe, 18.8. Found: C, 44.96; H, 3.42; Cl, 2.93; Fe, 18.7. IR (cm^{-1}): 3489 (w), 3099 (w), 1490 (s), 1428 (m), 1393 (s), 1355 (s), 1261 (m), 1108 (m), 1003 (m), 825 (m), 490 (s). $\mu_{eff} = 3.9\ \mu_B$.

$Ru_2(\mu\text{-fcac})_4Cl$ (2). This compound was prepared in a manner similar to **1** except that ferrocenylacetic acid (fcacH) was used (0.309 g, 1.26 mmol) and dissolved in 50 mL of hot methanol (instead of 30 mL). Refluxing was carried out for 8 h under argon. Yield = 0.189 g (74%). Mp = 210−212 °C (dec). Anal. Calcd (%) for $Ru_2Fe_4C_{48}H_{44}O_8Cl$: C, 47.65; H, 3.67; Cl, 2.93; Fe, 18.5. Found: C, 47.74; H, 3.72; Cl, 3.27; Fe, 18.6. IR (cm^{-1}): 3091 (w), 1467 (s), 1424 (s), 1393 (s), 1293 (m), 1104 (m), 1003 (m), 830 (s), 502 (s). $\mu_{eff} = 4.2\ \mu_B$.

$Ru_2(\mu\text{-fcp})_4Cl$ (3). This complex was prepared in a fashion similar to **2** except that 3-ferrocenylpropanoic acid (fcpH) was used (0.327 g, 1.26 mmol) and refluxing was carried out for 10 h. Yield = 0.241 g (83%). Mp = 200−202 °C (dec). Anal. Calcd (%) for $Ru_2Fe_4C_{52}H_{52}O_8Cl$: C, 49.33; H, 4.15; Cl, 2.80; Fe, 17.7. Found: C, 50.07; H, 4.18; Cl, 2.46; Fe, 17.4. IR (cm^{-1}): 3091 (w), 2925 (w), 1532 (m), 1463 (s), 1432 (s), 1413 (s), 1292 (w), 1104 (m), 1003 (s), 826 (s), 491 (s). $\mu_{eff} = 4.3\ \mu_B$.

(18) Cotton, F. A.; Donahue, J. P.; Lin, C.; Murillo, C. A. *Inorg. Chem.* **2001**, *40*, 1234.
(19) Cooke, M. W.; Murphy, C. A.; Cameron, T. S.; Swarts, J. C.; Aquino, M. A. S. *Inorg. Chem. Commun.* **2000**, *3*, 721.
(20) The Ru_2^{5+} core should best be viewed as a totally delocalized "valence-averaged" system with the extra electron distributed equally over the two rutheniums.
(21) Reeves, P. C. *Org. Synth.* **1977**, *56*, 29.
(22) Broadhead, G. D.; Osgerby, J. M.; Pauson, P. L. *J. Chem. Soc.* **1958**, 650.
(23) Rinehart, K. L.; Curby, R. J.; Sokol, P. E. *J. Am. Chem. Soc.* **1957**, *79*, 3420.
(24) Rausch, M. D.; Fisher, E. O.; Grubert, H. *J. Am. Chem. Soc.* **1960**, *82*, 76.
(25) Mitchell, R. W.; Spencer, A.; Wilkinson, G. *J. Chem. Soc., Dalton Trans.* **1973**, 846.
(26) Drysdale, K. D.; Beck, E. J.; Cameron, T. S.; Robertson, K. N.; Aquino, M. A. S. *Inorg. Chim. Acta* **1997**, *256*, 243.
(27) Figgis, B. N.; Nyholm, R. S. *J. Chem. Soc.* **1958**, 4190.

$Ru_2(\mu\text{-}O_2CCH_3)_3(\mu\text{-}fcb)Cl$ (4). Attempts to synthesize $Ru_2(\mu\text{-}fcb)_4Cl$ in a fashion similar to the complexes above proved unsuccessful due to the limited solubility of the 4-ferrocenylbutanoic acid (fcbH). Preparations using an 8−10-fold molar excess of fcbH, relative to the 0.100 g (0.21 mmol) of $Ru_2(\mu\text{-}O_2CCH_3)_4Cl$ starting material, in 200 mL of hot methanol followed by 16−24 h of reflux led to a complex that is most reasonably formulated as the tris-acetato-ferrocenylbutanoate derivative, $Ru_2(\mu\text{-}O_2CCH_3)_3(\mu\text{-}fcb)Cl$. This final product was extremely insoluble in most solvents, and subsequent dechlorination was not undertaken. Yield = 0.063 g (44%). Mp = 193−195 °C (dec). Anal. Calcd (%) for $Ru_2FeC_{20}H_{24}O_8Cl$: C, 35.02; H, 3.53; Cl, 5.17; Fe, 8.1. Found: C, 34.80; H, 3.45; Cl, 5.11; Fe, 8.3. IR (cm^{-1}): 3088 (w), 2929 (w), 2860 (w), 1540 (w), 1463 (s), 1416 (s), 1292 (w), 1104 (w), 1000 (m), 822 (m), 695 (m), 502 (s). $\mu_{eff} = 4.0\ \mu_B$.

$Ru_2(\mu\text{-}fcpe)_4Cl$ (5). This complex was prepared in a fashion similar to **3** except that 3-ferrocenyl-2-propenoic acid (fcpeH) was used (0.324 g, 1.26 mmol). Yield = 0.150 g (57%). Mp = 210−212 °C (dec). Anal. Calcd (%) for $Ru_2Fe_4C_{52}H_{44}O_8Cl$: C, 49.65; H, 3.53; Cl, 2.82; Fe, 17.8. Found: C, 49.67; H, 3.52; Cl, 3.07; Fe, 17.7. IR (cm^{-1}): 3088 (w), 2926 (w), 1625 (s), 1405 (s), 1393 (s), 1374 (s), 1288 (m), 1108 (w), 1000 (w), 973 (m), 822 (m), 506 (s). $\mu_{eff} = 4.2\ \mu_B$.

$Ru_2(\mu\text{-}rca)_4Cl$ (6). This compound was prepared similarly to **3** except that ruthenocenecarboxylic acid (rcaH) was used (0.349 g, 1.26 mmol). Yield = 0.240 g (86%). Mp = 220−222 °C (dec). Anal. Calcd (%) for $Ru_6C_{44}H_{36}O_8Cl$: C, 39.60; H, 2.72; Cl, 2.66; Ru, 45.4. Found: C, 39.48; H, 2.91; Cl, 2.75; Ru, 45.3. IR (cm^{-1}): 3107 (w), 2968 (w), 1629 (m), 1490 (s), 1393 (s), 1368 (m), 1104 (m), 1000 (m), 814 (m), 510 (s), 459 (s). $\mu_{eff} = 4.1\ \mu_B$.

$[Ru_2(\mu\text{-}fca)_4(EtOH)_2](PF_6)$ (7). The formation of all the adducts was achieved by dechlorination of the corresponding chloride complexes under argon. Typically 0.050 g (0.042 mmol) of **1** and 0.011 g (0.042 mmol) of $AgPF_6$ were suspended in 80 mL of thoroughly degassed ethanol or 1-propanol. The suspension was stirred at 40−50 °C for 1 h. Initially the solution is faint red in color but slowly darkens as more dechlorination takes place and more of the adduct is formed. The solution was then filtered over Celite (to remove the AgCl) and the filtrate evaporated to dryness, yielding a microcrystalline red-brown product. Yield = 0.056 g (98%). Mp = 218−220 °C (dec). Crystals suitable for X-ray diffraction[19] could be obtained by slow evaporation of a 1-propanol solution of the adduct. Crystals could also be obtained from methanol or ethanol; however, they were hampered by solvent loss during the diffraction process. Anal. Calcd (%) for $Ru_2Fe_4C_{48}H_{48}O_{10}PF_6$ (ethanol adduct): C, 42.54; H, 3.57; Fe, 16.5. Found: C, 42.44; H, 3.59; Fe, 16.9. IR (cm^{-1}): 3508 (m), 3111 (w), 2972 (w), 1614 (m), 1490 (s), 1420 (s), 1393 (s), 1355 (s), 1290 (m), 1108 (m), 1003 (m), 841 (s), 494 (s), 482 (s). $\mu_{eff} = 4.0\ \mu_B$.

$[Ru_2(\mu\text{-}fcac)_4(1\text{-propanol})_2](PF_6)$ (8). This adduct was prepared in a fashion similar to **7** except that the chloride salt **2** was used and the suspension allowed to stir for 2 h. The extra time was required for complete dechlorination since the solubility of the chloride complexes diminishes as the number of methylene groups increases. Yield = 0.041 g (70%). Mp = 148−150 °C (dec). Anal. Calcd (%) for $Ru_2Fe_4C_{54}H_{60}O_{10}PF_6$ (1-propanol adduct): C, 45.05; H, 4.21; Fe, 15.5. Found: C, 45.07; H, 3.95; Fe, 15.1. IR (cm^{-1}): 3470 (m), 3095 (w), 2972 (w), 1640 (m), 1463 (s), 1424 (s), 1393 (s), 1285 (m), 1108 (m), 1003 (m), 845 (s), 506 (s), 486 (s). $\mu_{eff} = 4.1\ \mu_B$.

$[Ru_2(\mu\text{-}fcp)_4(1\text{-propanol})_2](PF_6)$ (9). This complex was prepared in a fashion similar to **7** except that the chloride salt **3** was used and the suspension allowed to stir for 3 h. Yield = 0.050 g (94%). Mp = 118−120 °C. Anal. Calcd (%) for $Ru_2Fe_4C_{58}H_{68}O_{10}PF_6$ (1-propanol adduct): C, 46.57; H, 4.59; Fe, 14.9. Found: C, 46.43; H, 4.25; Fe, 14.7. IR (cm^{-1}): 3470 (m), 3095 (w), 2929 (w), 1633 (w), 1540 (m), 1463 (s), 1432 (s), 1416 (s), 1278 (m), 1104 (m), 1003 (m), 841 (s), 502 (m), 486 (s). $\mu_{eff} = 4.2\ \mu_B$.

$[Ru_2(\mu\text{-}fcpe)_4(1\text{-propanol})_2](PF_6)$ (10). The solubility of the chloride salt, **5**, in ethanol was relatively good, and the adduct could be prepared in the same manner as **7** with only 1 h of stirring needed to complete the dechlorination. Yield = 0.045 g (74%). Mp = 215−217 °C. Crystals suitable for X-ray diffraction could be obtained by slow evaporation of a 1-propanol solution of **10**. Anal. Calcd (%) for $Ru_2Fe_4C_{58}H_{60}O_{10}PF_6$ (1-propanol adduct): C, 45.73; H, 3.98; Fe, 14.7. Found: C, 46.08; H, 3.96; Fe, 15.1. IR (cm^{-1}): 3470 (w), 3099 (w), 2964 (w), 1621 (s), 1441 (m), 1405 (s), 1389 (s), 1374 (s), 1285 (s), 1108 (w), 1003 (w), 973 (w), 853 (s), 501 (m). $\mu_{eff} = 4.1\ \mu_B$.

$[Ru_2(\mu\text{-}rca)_4(EtOH)_2](PF_6)$ (11). For the preparation of **11** methanol and ethanol were the preferred solvents over 1-propanol. Due to the limited solubility of **6**, only 0.030 g (0.023 mmol) was used and therefore only 0.0057 g (0.023 mmol) of $AgPF_6$. The dechlorination process was complete in about 1 h when methanol was used or about 4 h for ethanol. 1-Propanol required even longer stirring times. Yield = 0.030 g (88%). Mp = 208−210 °C. Crystals suitable for X-ray diffraction were obtained by slow evaporation of a 1-propanol solution of **11**. Anal. Calcd (%) for $Ru_6C_{48}H_{48}O_{10}PF_6$ (ethanol adduct): C, 37.53; H, 3.15; Ru, 39.5. Found: C, 37.78; H, 3.23; Ru, 39.8. IR (cm^{-1}): 3508 (m), 3107 (w), 2976 (w), 1633 (w), 1490 (s), 1389 (s), 1370 (m), 1100 (m), 1000 (m), 849 (s), 513 (s). $\mu_{eff} = 4.1\ \mu_B$.

X-ray Crystallography. Crystals of compounds **1**, **10**, and **11** were mounted in glass capillaries, and all measurements were made on a Mercury CCD area detector coupled with a Rigaku AFC8 diffractometer with graphite-monochromated Mo Kα radiation. Data were collected and processed using CrystalClear (Rigaku).[28] The structures were solved by direct methods[29] and expanded using Fourier techniques.[30] For all the complexes some non-hydrogen atoms were refined anisotropically, while the rest were refined isotropically. Hydrogen atoms were included but not refined. For complex **1** see further below. In complex **10** the carbon atoms C(41) and C(42) in one of the ethylene chains were found to be disordered over two positions with occupancies of 50% each. Two of the three 1-propanol solvent molecules were also found to be disordered. The final cycle of full-matrix least-squares refinement on F^2 was based on 14 348 observed reflections ($I > 2\sigma(I)$) and 800 variable parameters. For complex **11** the final cycle of full-matrix least-squares refinement on F was based on 794 observed reflections ($I > 3\sigma(I)$) and 148 variable parameters. All calculations were performed using the teXsan crystallographic software package of Molecular Structure Corporation.[31]

Results and Discussion

Synthesis. The desired tetrametallocenecarboxylate compounds could be readily prepared by an often used carboxylate exchange reaction[31] in which $Ru_2(\mu\text{-}O_2CCH_3)_4Cl$ is reacted with an excess (normally 6- to 8-fold) of the desired metallocenecarboxylic acid (see Chart 1) in a refluxing alcohol (usually methanol, ethanol, or 1-propanol) under air-free conditions to form the chloride derivatives **1**−**6**. These are subsequently dechlorinated by reaction with $AgPF_6$ to give the

(28) *CrystalClear*: Rigaku Corporation, 1999.
(29) *SHELXS86*: Sheldrick, G. M. In *Crystallographic Computing 3*; Sheldrick, G. M., Kruger, C., Goddard, R., Eds.; Oxford University Press, 1985; pp 175−189.
(30) *DIRDIF94*: Beurskens, P. T.; Admiraal, G.; Beurskens, G.; Bosman, W. P.; de Gelder, R.; Israel, R.; Smits, J. M. M. *The DIRDIF-94 program system*; Technical Report of the Crystallography Laboratory; University of Nijmegen: The Netherlands, 1994.
(31) *TeXsan for Windows version1.06*, Crystal Structure Analysis Package; Molecular Structure Corporation, 1997−1999.

significantly more soluble di-alcohol adducts as hexafluorophosphate salts **7**−**11**. An example of the two-step reaction sequence is given below using fcaH as the carboxylic acid.

$$Ru_2(\mu\text{-}O_2CCH_3)_4Cl + 4\ fcaH \xrightarrow[ROH]{\Delta} Ru_2(\mu\text{-}fca)_4Cl + 4\ CH_3CO_2H \quad (I)$$

$$Ru_2(\mu\text{-}fca)_4Cl + AgPF_6 \xrightarrow[ROH]{} [Ru_2(\mu\text{-}fca)_4(ROH)_2](PF_6) + AgCl \quad (II)$$

It should be noted, however, as the saturated chain length between the carboxylic acid group and the Cp ring increases, the solubilities in alcohols of both the free acids and the diruthenium chloride derivatives decrease. As a consequence, initial refluxing times were increased (to ensure complete exchange) and dechlorination times were also extended to ensure a higher yield of the final di-adduct product. Unfortunately 4-ferrocenylbutanoic acid had such limited solubility in our reaction solvents that it appears only a monosubstituted derivative (**4**) could be isolated as a chloride salt. The subsequent dechlorination reaction was not performed, as **4** is essentially insoluble in all but the most strongly donating solvents. While complexes **2**, **3**, and **6** also suffered from poor solubilities, we were able to carry out the dechlorination process. Two of the subsequent di-adduct products, **8** and **9**, showed sufficient solubilities even in noncoordinating solvents to allow electrochemical measurements. However, the ruthenocene carboxylate derivative, **11**, was only sufficiently soluble in stronger donors, and we were forced to use *N*,*N*′-dimethylformamide for our electrochemical measurements on this adduct. Satisfactory elemental analyses were obtained for all complexes, with complex **4** having a formulation that is most likely $Ru_2(\mu\text{-fcb})(\mu\text{-}O_2CCH_3)_3Cl$.

IR Spectroscopy. Common to the IR spectra of all the complexes are modes associated with the metallocenyl moiety, with those bands in the fingerprint regions being particularly diagnostic. According to Nakamoto,[33] for ferrocene and ruthenocene, these include the asymmetric ring-tilt at 492 and 450 cm^{-1}, respectively, along with the asymmetric metal-to-ring stretching at 478 and 380 cm^{-1}, respectively, the values for the ruthenocene being lower in both cases. For our ferrocenecarboxylate derivatives the ring-tilt mode is seen in the range 490−506 cm^{-1} and the metal-to-ring stretching between 478 and 486 cm^{-1}. In the case of the ruthenocenecarboxylate derivative one of these modes occurs, as expected, at lower frequencies with the asymmetric ring-tilt occurring at 459 cm^{-1} in the chloride complex **6**. We were not able to detect the stretching mode, as it was beyond the limit of our instrument.

Other characteristic bands, for both the chloride complexes and the di-adducts, include the asymmetric and symmetric carboxylate stretches. The former is found in the range 1441−1490 cm^{-1} and the latter from 1389 to 1416 cm^{-1}. The difference in the ν_{asym}(COO) and ν_{sym}(COO) values, or $\Delta\nu$, is diagnostic of the type of OCO binding that is occurring, i.e., monodentate, bidentate, or bridging. The values of $\Delta\nu$ in all of our complexes range from 50 to 100 cm^{-1}, consistent with a bridging mode of coordination.[33] The chloride complexes **1**−**6** are easily differentiated from the di-adduct PF_6^- salts **7**−**11** by the strong $\nu(PF_6^-)$ at around 845 cm^{-1} seen for the latter. The stereochemistry of the fcpe derivative (which is clearly seen to be *trans* from the crystal structure discussed below) appears to be *trans* in the IR as well, due to the very weak intensity of the C−H bending mode (for a 1,2-disubstituted double bond) at 973 cm^{-1}.

Electronic and Magnetic Properties. The UV−visible spectra of all the complexes were run in alcohol and are rather complicated but predominated (particularly in the UV) by bands characteristic of the metallocene moieties, as there are four of these to every one dimeric ruthenium unit. In fact, the position of the bands in the free metallocene carboxylic acids are very similar to the positions of the bands in the starting diruthenium tetraacetate chloride, $Ru_2(\mu\text{-}O_2CCH_3)_4Cl$. The free metallocene acids have d−d bands at about 440 nm ($^1A_{1g} \rightarrow {}^1E_{1g}$) and 330 nm ($^1A_{1g} \rightarrow {}^1E_{2g}$) and an LMCT band at about 220 nm ($^1A_{1g} \rightarrow {}^1A_{2u}$),[34] whereas $Ru_2(\mu\text{-}O_2CCH_3)_4Cl$ has bands at about 425 nm (π(Ru−O, Ru_2) → $\pi^*(Ru_2)$), 320 nm (π(Cl) → $\pi^*(Ru_2)$), and about 225 nm, which has not been assigned but is presumably ligand based.[32] The net result for the tetrametallocene complexes is very strong absorptions in all three of these regions with significant overlap of bands due to the metallocene and diruthenium-core moieties. A more detailed study of the electronic spectra (including the near-infrared region) of these complexes as well as spectroelectrochemical measurements of the oxidized and reduced species is currently being undertaken and will be the subject of a separate paper.

Magnetic susceptibility measurements performed at room temperature gave values of 3.9−4.3 μ_B for all 11 complexes. This is consistent with the presence of three unpaired electrons per dimer unit, as is common for these mixed-valent tetracarboxylate systems.[32]

X-ray Structures. The limited solubilities of the chloride derivatives hampered our crystal-growing efforts. We were able to obtain single crystals only for the $Ru_2(\mu\text{-fca})_4Cl$ derivative **1**. Crystals obtained from 1,2-dichloroethane degraded too rapidly, even at low temperatures, for sufficient data collection. When 1,1,2,2-tetrachlorethane was used, the lifetime of the crystal was extended, but crystal integrity was still a problem and final refinement was very poor. Only a "rough" structure could be obtained (see below). As mentioned, the solubilities of the di-adducts were significantly better, and structures of $[Ru_2(\mu\text{-fca})_4(1\text{-propanol})_2](PF_6)$ (**7**), previously reported,[19] $[Ru_2(\mu\text{-fcpe})_4(1\text{-propanol})_2](PF_6)$ (**10**), and $[Ru_2(\mu\text{-rca})_4(1\text{-propanol})_2](PF_6)$ (**11**) were obtained. The use of the higher boiling solvent 1-propanol (as opposed to ethanol or methanol) for recrystallization yielded crystals in which solvent loss was not a significant problem during data collection.

The pertinent crystallographic details for **10** and **11** are given in Table 1.

$Ru_2(\mu\text{-fca})_4Cl$ (1). Due to the very poor nature of this structure,[35] we can only comment qualitatively. It is

(32) Aquino, M. A. S. *Coord. Chem. Rev.* **1998**, *170*, 141.
(33) Nakamoto, K. *Infrared and Raman Spectra of Inorganic and Coordination Compounds*, Part B, 5th ed.; Wiley Inter-Science: New York, 1997.
(34) Long, N. J. *Metallocenes: Introduction to Sandwich Complexes*; Blackwell: London, 1998.

Table 1. Crystal Data and Structure Refinement for $[Ru_2(\mu\text{-fcpe})_4(1\text{-propanol})_2](PF_6)\cdot 3(1\text{-propanol})$ (10) and $[Ru_2(\mu\text{-rca})_4(1\text{-propanol})_2](PF_6)\cdot(1\text{-propanol})$ (11)

empirical formula	$C_{67}H_{82}O_{13}PF_6Fe_4Ru_2$ (**10**)	$C_{53}H_{57}O_{11}PF_6Ru_6$ (**11**)
fw	1665.84	1621.41
space group (No.)	$P\bar{1}$ (2)	$P\bar{1}$ (2)
a (Å)	12.4199 (10)	9.490 (3)
b (Å)	15.3462 (2)	11.835 (4)
c (Å)	20.756 (2)	14.718 (4)
α (deg)	78.366 (5)	61.46 (1)
β (deg)	77.653 (6)	71.79 (2)
γ (deg)	68.928 (5)	82.66 (2)
V (Å^3)	3572.2 (6)	1379.1 (8)
Z	2	1
T (°C)	−130	−90
wavelength (Å)	0.71069	0.71069
d_{calcd} (g cm^{-3})	1.549	1.952
abs coeff (mm^{-1})	1.299	1.709
$R_1[I > 2\sigma(I)]^a$	0.0649	
$wR_2{}^b$	0.1058	
$R[I > 3\sigma(I)]^c$		0.079
$R_w{}^d$		0.095

[a] $R_1 = \sum||F_o| - |F_c||/\sum|F_o|$. [b] $wR_2 = [\sum w(F_o^2 - F_c^2)^2/\sum w(F_o^2)^2]^{1/2}$. [c] $R = \sum||F_o| - |F_c||/\sum|F_o|$. [d] $R_w = [\sum w(|F_o| - |F_c|^2/\sum wF_o^2]^{1/2}$.

Chart 2

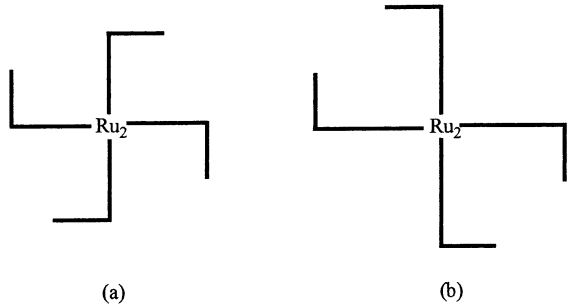

clear that there are four ferrocenecarboxylates surrounding a diruthenium core. A chloride is present in one of the axial positions with an unidentified molecule in the other axial site. It is not entirely clear what this molecule is (perhaps a disordered 1-propanol), but it is clear that the compound is not polymeric, as most of the previous diruthenium tetracarboxylate chloride structures have been.[32] The axial chloride does not bridge an adjacent diruthenium unit. Structures of nonpolymeric chloride derivatives have recently been reported by Barral.[36] In addition there are four 1,1,2,2-tetrachloroethane molecules of solvation present displaying varying degrees of disorder.

$[Ru_2(\mu\text{-fcpe})_4(1\text{-propanol})_2](PF_6)$ (10). Compound **10** crystallizes in a primitive triclinic system ($P\bar{1}$). Selected bond lengths and angles are listed in Table 2. An ORTEP diagram of the complex is shown in Figure 1. Despite some disorder in the ethylene spacer linking one of the carboxyl groups to the ferrocenyl group (C(4)−C(41AB)−C(42AB)−C(43)), the structure clearly shows the four *trans*-3-ferrocenyl-2-propenate groups bridging the diruthenium core. In contrast to the structure of $[Ru_2(\mu\text{-fca})_4(1\text{-propanol})_2](PF_6)$ (**7**),[19] the pendant ferrocenyls are grouped in two pairs (i.e., two adjacent ferrocenyls) facing each other. When viewed along the Ru−Ru bond axis, the skeletal shape of the complex looks like two incomplete squares joined at a corner (see (b) in Chart 2). In **7** each adjacent ferrocenyl is pointing away from its neighbor, and this structure when viewed down the Ru−Ru axis has a skeletal swastika-like shape ((a) in Chart 2). This difference is probably due to the decrease in steric crowding that occurs as the chain length between carboxyl group and ferrocenyl increases, allowing for greater freedom of rotation around the Cp carbon−chain carbon bond. The skeletal structure of **11**, as might be expected, is the same as **7** and adopts the (a) conformation. The structure of **10** also shows that three of the four ferrocenyl groups (we ignore the fourth ferrocenyl for now, as it is attached to the disordered ethylene spacer) have Cp rings that deviate by only 2−4° from the eclipsed conformation. This deviation is less than what was found in complex **7** (8−16°).[19] The average deviation in the fourth ferrocenyl group is about 13°.

Table 2. Selected Bond Lengths (Å) and Angles (deg) for $[Ru_2(\mu\text{-fcpe})_4(1\text{-propanol})_2](PF_6)\cdot 3(1\text{-propanol})$ (10)

Ru(1)−Ru(2)	2.262(2)	Ru(1)−O(9)	2.276(12)
Ru(2)−O(10)	2.267(11)	Ru(1)−O(5)	1.992(9)
Ru(1)−O(3)	2.014(8)	Ru(1)−O(7)	2.023(10)
Ru(1)−O(1)	2.026(8)	Ru(2)−O(8)	2.003(10)
Ru(2)−O(4)	2.007(8)	Ru(2)−O(2)	2.033(9)
Ru(2)−O(6)	2.043(9)	O(1)−C(1)	1.28(2)
O(2)−C(1)	1.23(2)	O(9)−C(53)	1.430(12)
O(10)−C(56)	1.414(12)	C(1)−C(5)	1.49(2)
C(3)−C(29)	1.53(2)	C(5)−C(6)	1.313(11)
C(6)−C(7)	1.48(2)	C(7)−C(11)	1.39(2)
Fe(1)−C(12)	2.03(2)	Fe(1)−C(7)	2.032(11)
Fe(1)−C(11)	2.029(12)		
Ru(2)−Ru(1)−O(9)	178.0(3)	O(5)−Ru(1)−O(3)	89.0(4)
O(5)−Ru(1)−O(7)	179.0(5)	O(3)−Ru(1)−O(7)	90.8(3)
O(5)−Ru(1)−O(1)	92.2(3)	O(8)−Ru(2)−O(4)	91.2(3)
O(8)−Ru(2)−O(2)	88.4(4)	O(4)−Ru(2)−O(2)	179.4(4)
O(4)−Ru(2)−O(6)	87.7(3)	Ru(1)−Ru(2)−O(10)	176.7(3)
C(1)−O(1)−Ru(1)	118.3(9)	C(1)−O(2)−Ru(2)	117.7(9)
O(2)−C(1)−O(1)	124.6(12)	O(2)−C(1)−C(5)	121.2(13)
C(6)−C(5)−C(1)	121.8(13)	C(5)−C(6)−C(7)	124.5(12)
C(8)−C(7)−C(6)	125.9(11)	C(6)−C(7)−Fe(1)	122.4(8)
C(8)−C(7)−Fe(1)	69.3(7)	C(53)−O(9)−Ru(1)	115.2(10)

The Ru−Ru, Ru−O_{eq}, and Ru−O_{ax} bond lengths as well as the core bond angles in **10** are typical for these types of compounds.[32] The double bond in the 2-propenoate group is maintained (and hence so is the conjugation), as can be seen from the spacer−chain bond lengths, for example, C(1)−C(5) = 1.49(2) Å, C(5)−C(6) = 1.31(1) Å, and C(6)−C(7) = 1.48(2) Å. The average through-bond distance between remote Fe sites, either *cis* or *trans* to each other, is 19.3(2) Å, 5.8 Å longer than for the corresponding distance in complex **7**.

$[Ru_2(\mu\text{-rca})_4(1\text{-propanol})_2](PF_6)$ (11). Compound **11** crystallizes in a primitive triclinic cell ($P\bar{1}$) with a center of inversion lying halfway along the Ru−Ru bond. This is the first structurally characterized complex containing ruthenocenecarboxylate, as a ligand, that we are aware of. Selected bond lengths and angles are listed

(35) **1** crystallizes in a primitive triclinic unit cell, $P\bar{1}$, with cell dimensions a = 13.289(4) Å, b = 13.604(5) Å, c = 20.559(7) Å, α = 90.388(9)°, β = 76.688(5)°, γ = 65.816(3)°. V = 3277.8(17) Å^3, Z = 4, and fw = 844.00 with a calculated density of 1.71 g/cm^3. Of the 36 800 reflections that were collected, 16 118 were unique (R_{int} = 0.148). The final cycle of full-matrix least-squares refinement on F^2 was based on 6372 observed reflections and 425 variable parameters and converged (largest parameter shift was 0.008 times its esd) with unweighted and weighted agreement factors of R_1 = 0.081 and wR_2 = 0.229.

(36) (a) Barral, M. C.; Jiménez-Aparicio, R.; Priego, J. L.; Royer, E. C.; Urbanos, F. A.; Amador, U. *J. Chem. Soc., Dalton Trans.* **1997**, 863. (b) Barral, M. C.; Jiménez-Aparicio, R.; Priego, J. L.; Royer, E. C.; Urbanos, F. A.; Amador, U. *Inorg. Chem.* **1998**, *37*, 1413.

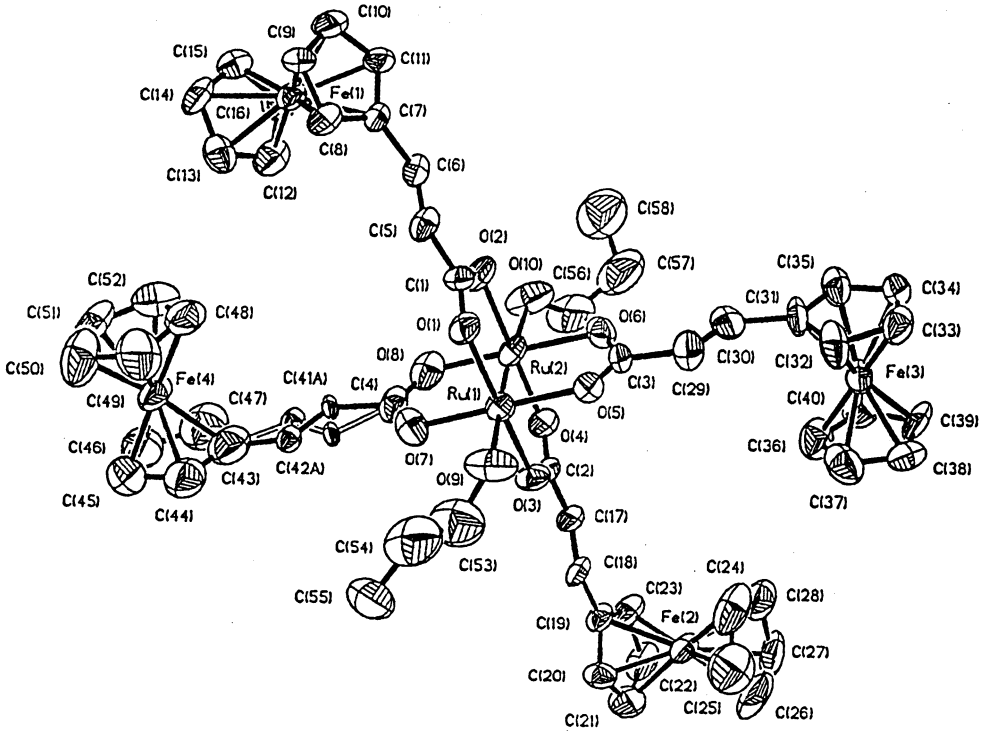

Figure 1. ORTEP diagram of the cation of complex **10**. Disorder can be seen in the spacer of one of the bridging ligands. 1-Propanol molecules of solvation and PF_6^- counterion are omitted for clarity.

Table 3. Selected Bond Lengths (Å) and Angles (deg) for $[Ru_2(\mu\text{-rca})_4(1\text{-propanol})_2](PF_6)\cdot(1\text{-propanol})$ (11)

Ru(1)−Ru(1A)	2.260(10)	Ru(1)−O(5)	2.27(3)
Ru(1)−O(1)	2.03(3)	Ru(1)−O(2)	2.03(3)
Ru(1)−O(3)	2.00(3)	Ru(1)−O(4)	1.99(3)
O(1)−C(1)	1.26(6)	O(2A)-C(1)	1.29(6)
O(3)−C(2)	1.35(6)	O(4A)-C(2)	1.29(5)
C(1)−C(3)	1.37(7)	C(2)−C(13)	1.37(7)
O(5)−C(23)	1.45(6)	C(13)−C(14)	1.37(7)
Ru(2)−C(19)	2.13(7)	Ru(3)−C(10)	2.12(5)
Ru(1A)−Ru(1)−O(1)	90.0(8)	Ru(1A)−Ru(1)−O(2)	88.9(9)
Ru(1A)−Ru(1)−O(3)	91.4(9)	Ru(1A)−Ru(1)−O(4)	91.5(8)
Ru(1A)−Ru(1)−O(5)	175.7(9)	O(1)−Ru(1)−O(2)	177.7(9)
O(1)−Ru(1)−O(3)	88.9(9)	O(1)−Ru(1)−O(4)	89.5(9)
O(1)−Ru(1)−O(5)	88.8(9)	O(2)−Ru(1)−O(3)	89.1(9)
O(2)−Ru(1)−O(4)	92.5(9)	O(2)−Ru(1)−O(5)	92.5(9)
O(3)−Ru(1)−O(4)	176.8(9)	O(3)−Ru(1)−O(5)	92.8(8)
O(4)−Ru(1)−O(5)	84.4(9)	Ru(1)−O(1)−C(1)	119(3)
Ru(1)−O(2)−C(1A)	121(3)	Ru(1)−O(3)−C(2)	115(3)
Ru(1)−O(4)−C(2A)	115(3)	Ru(1)−O(5)−C(23)	122(3)
O(1)−C(1)−O(2A)	122(5)	O(1)−C(1)−C(3)	117(5)
O(2A)−C(1)−C(3)	121(4)	O(3)−C(2)−O(4A)	127(4)
O(3)−C(2)−C(13)	115(3)	O(4A)−C(2)−C(13)	117(4)
C(1)−C(3)−C(4)	135(5)	C(1)−C(3)−C(7)	134(5)
C(2)−C(13)−Ru(2)	118(3)	C(1)−C(3)−Ru(3)	127(4)
C(13)−Ru(2)−C(17)	36(2)	C(3)−Ru(3)−C(4)	40(2)

in Table 3. An ORTEP diagram is shown in Figure 2. As mentioned above when viewed along the Ru−Ru axis, the skeletal structure of **11** is the same as **7** and resembles the swastika-like form in Chart 1(a). The conformations of the Cp rings on the two unique ruthenocenyl groups deserve mention as, unlike **7** and **10**, there is essentially a mixture of eclipsed and staggered forms with the rings attached to Ru(3) (and hence Ru(3A)) showing an eclipsed conformation with a deviation of 1.6° and the rings attached to Ru(2) (and Ru(2A)) being closer to a staggered conformation with a deviation of 23° from eclipsed. We are not sure why this should be the case but do note that the PF_6^- counterion lies significantly closer to the Ru(2) (and Ru(2A))-containing ruthenocenyl group than the others. Since we are always loath to blame unexplained crystal structure phenomena on packing forces, in this case they may play a role.

The Ru−Ru, Ru−O_{eq}, and Ru−O_{ax} bond lengths as well as the core bond angles are all typical for these types of compounds.[32] In this case the average through-bond distance for remote Ru sites (either *cis* or *trans*) is 13.9(2) Å. This is slightly longer but comparable to the through-bond Fe−Fe distance in complex **7** (13.5 Å).[19] There is no significant hydrogen-bonding to speak of.

Electrochemistry. Electrochemical measurements were carried out on the free acids and the complexes. Since the chloride complexes of the ferrocenyl-containing derivatives **1**−**5** were not sufficiently soluble in the noncoordinating solvents dichloromethane and 1,2-dichloroethane, all measurements were made on the di-adduct complexes **7**−**10**. *Neither* of the ruthenocenoic acid derivatives **6** or **11** were soluble in these noncoordinating solvents. Consequently measurements had to be performed in *N*,*N*′-dimethylformamide (DMF). The electrochemistry of the free acids, the ferrocene derivatives, and the ruthenocene derivative will now be discussed in turn.

Free Acids. Cyclic voltammetry was performed on all of the ferrocenecarboxylic acids (except 4-ferrocenylbutanoic acid due to low solubility) in 1,2-dichloroethane (DCE). In all cases a one-electron, reversible or quasi-reversible, redox process was observed corresponding to the $Fe^{3+/2+}$ couple. The values for the four ferrocenecarboxylic acids (vs Fc^+/Fc) are summarized in Table 4 along with values for three of them determined in the coordinating solvent acetonitrile (vs SCE)

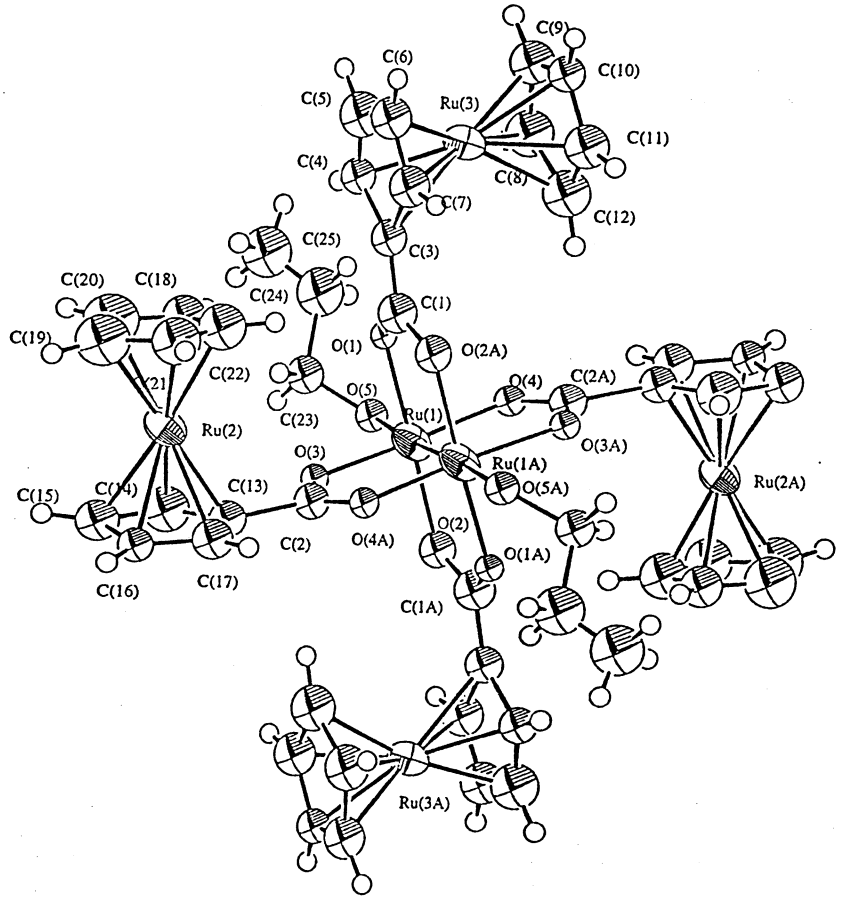

Figure 2. ORTEP diagram of the cation of complex **(11)**. 1-Propanol molecule of solvation and PF_6^- counterion are omitted for clarity.

Table 4. Reduction Potentials for the Free Metallocenecarboxylic Acids

free acid	$E_{1/2}$ (mV vs Fc^+/Fc)[a]	$E_{1/2}$ (mV vs SCE)[b]
fcaH	234	570
fcacH	50	340
fcpH	38	310
fcpeH	127	
rcaH[c]	393[d]	

[a] In 1,2-dichloroethane (0.100 M TBAH) at 25 °C. Scan rate = 100 mV s^{-1}. [b] In acetonitrile (0.100 M $LiClO_4$) at 25 °C. Scan rate = 100 mV s^{-1} (ref 37). [c] In *N*,*N*′-dimethylformamide (0.100 M TBAH) at 25 °C. Scan rate = 100 mV s^{-1}. [d] Anodic peak (E_a) only.

by Blom et al.[37] The electron-withdrawing ability of the carboxyl group serves to raise the potential above that of the free ferrocene value; however, the electron-donating ability of the increasing number of methylene spacer groups serves to partially cancel the electron-withdrawing inductive effect of the carboxyl group and bring the redox potential closer to the value of free ferrocene. This decreasing trend is seen in both sets of measurements. Introducing conjugation between the Cp ring and the carboxyl group serves to partially remediate the electron-withdrawing effect and raise the redox potential again for fcpeH in our measurements in DCE.

Due to the limited solubility of rcaH, measurements were carried out in the moderately strong donor solvent DMF. RcaH displays an irreversible (no E_c observed) oxidation process, with E_a = 393 mV (vs Fc^+/Fc). This is assigned to a one-step two-electron oxidation in accordance with the results previously reported by Kuwana et al.[38] They observed a value of 0.693 V vs SCE for this process with ferrocene falling at 0.307 V vs SCE (in acetonitrile with 0.2 M $LiClO_4$). This yields a value of 0.386 V vs Fc^+/Fc, which is in good agreement with our value above.

Diruthenium Ferrocenecarboxylate Derivatives 7−10. Extensive cyclic voltammetry (CV) and Osteryoung square-wave voltammetry (OSWV) were performed on complex **7** in our preliminary communication.[19] A few aspects of that study are worth reviewing here. In the cyclic voltammogram an irreversible one-electron reduction ($E_c \approx -760$ mV vs Fc^+/Fc) was observed corresponding to the core $Ru_2^{5+/4+}$ couple as well as four partially superimposed one-electron ferrocenyl-centered redox processes (coulometry indicates a total of four electrons). The existence of ferrocenyl-based mixed-valent intermediate states possessing both Fe^{II} and Fe^{III} sites was implied by the splitting of the ferrocenyl wave into two observable cathodic and anodic peaks (i.e., each peak corresponding to two closely overlapping one-electron transfer processes). This splitting of redox waves was also seen in the OSWV experiments where two peaks, each of which corresponded to two closely overlapping one-electron-transfer processes, were observed. Splittings observed

(37) Blom, N. F.; Neuse, E. W.; Thomas, H. G. *Trans. Met. Chem.* **1987**, *12*, 301.

(38) Kuwana, T.; Bublitz, D. E.; Hoh G. *J. Am. Chem. Soc.* **1960**, *82*, 5811.

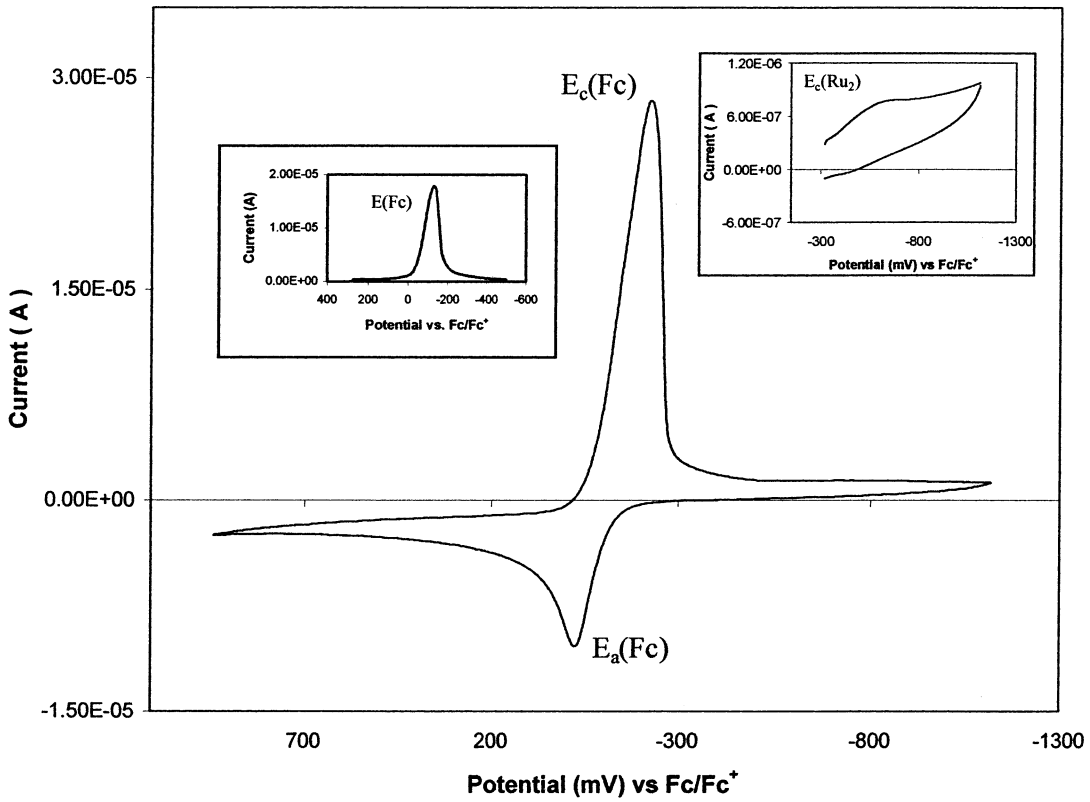

Figure 3. Cyclic voltammogram of complex **9** in 1,2-dichloroethane (0.100 M TBAH) at a scan rate of 100 mV s^{-1} vs Fc^+/Fc (25 °C). Inset top left: Osteryoung square-wave voltammogram showing the ferrocenyl-centered redox process (E(Fc)). No splitting is seen. Inset top right: $Ru^{II}Ru^{III}$ reduction ($E_c(Ru_2)$).

Table 5. CV and OSWV Electrochemical Data for Complexes 7−11[a]

complex	E_c(Mc)[b]	ΔE_c(Mc)	E_a(Mc)[c]	ΔE_a(Mc)	E(Mc)[d]	ΔE(Mc)	$E_c(Ru_2)$	$E(Ru_2)$	i_c/i_a[e]
(**7**) (fca)	60, −20	80	112, 25[f]	87	82, 4	78	−758	−659	4.0
(**8**) (fcac)	−140		14		−59		*g*	*g*	3.1
(**9**) (fcp)	−225		−25		−132		−647	−603	2.9
(**10**) (fcpe)	−62		84		33, −8	41	−863	−778	1.6
(**11**)[h] (rca)	*g*		374		287		−550	−516	

[a] All measurements (except for complex **11**) carried out in 1,2-dichloroethane at 25 °C with 0.100 M TBAH at a scan rate of 100 mV s^{-1}. All entries are given in mV vs Fc^+/Fc. E_c, E_a, ΔE_c, and ΔE_a values are from CV measurements. E and ΔE values are from OSWV measurements. Mc = metallocene-based redox process. Ru_2 = core diruthenium redox process. [b] Where two values are reported, this indicates a "splitting" of the CV oxidation wave. For complex **7** the two values correspond to E_{c1} and E_{c2} in ref 19. [c] Where two values are reported, this indicates a "splitting" of the CV reduction wave. For complex **7** the two values correspond to E_{a1} and E_{a2} in ref 19. [d] Where two values are reported, this indicates a "splitting" in the OSWV wave. For complex **7** the two values correspond to E_{f1} and E_{f2} in ref 19. [e] Cathodic to anodic peak current ratios from the CV for the metallocenyl-centered process. [f] Measured at 500 mV s^{-1} (no unambiguous peak was seen at 100 mV s^{-1}, ref 19). [g] No clear peak observed. [h] In DMF at 25 °C with 0.100 M TBAH at a scan rate of 100 mV s^{-1}.

from both techniques ranged from 75 to 90 mV. From this CV and OSWV evidence it was concluded that there was small but significant intra-ferrocenyl communication occurring. An additional feature of the cyclic voltammogram was the inordinately large cathodic to anodic peak current ratios (i_c/i_a) which was attributed to substrate deposition at the working electrode. A similar phenomenon was observed by Lever and co-workers in a tetraferrocenyl-phthalocyanine derivative.[39]

In the present work on the ferrocenecarboxylate derivatives **8**−**10** we sought to investigate two additional and important aspects of these systems. How would increasing the distance between Fe sites by introducing (a) saturated spacers and (b) unsaturated (conjugated) spacers affect the electrochemical properties (and hence any potential ferrocenyl−ferrocenyl communication) in these systems? The cyclic voltammogram of **9** (Figure 3) clearly shows, when scanning in an oxidizing direction from −200 mV, a wave (E_a(Fc) = −25 mV vs Fc^+/Fc) corresponding to the four electrons from the ferrocenyl irons. Some deposition then occurs as the fully oxidized species is less soluble than the reduced complex, and upon scanning in the reducing direction, a larger peak (E_c(Fc) = −225 mV vs Fc^+/Fc) is observed corresponding to rereduction (four electrons) of the ferrocenyl groups. The shape of this entire process is essentially identical to that observed by Lever and co-workers[39] as mentioned above. When scanning in the reducing direction, a weak irreversible one-electron reduction process is seen ($E_c(Ru_2)$ = −647 mV vs Fc^+/Fc). This corresponds to the core $Ru_2^{5+/4+}$ couple (see right inset in Figure 3). The OSWV for complex **9** shows a ferrocenyl-centered process with a single peak,

(39) Jin, Z.; Nolan, K.; McArthur, C. R.; Lever, A. B. P., Leznoff, J. *J. Organomet. Chem.* **1994**, *468*, 205.

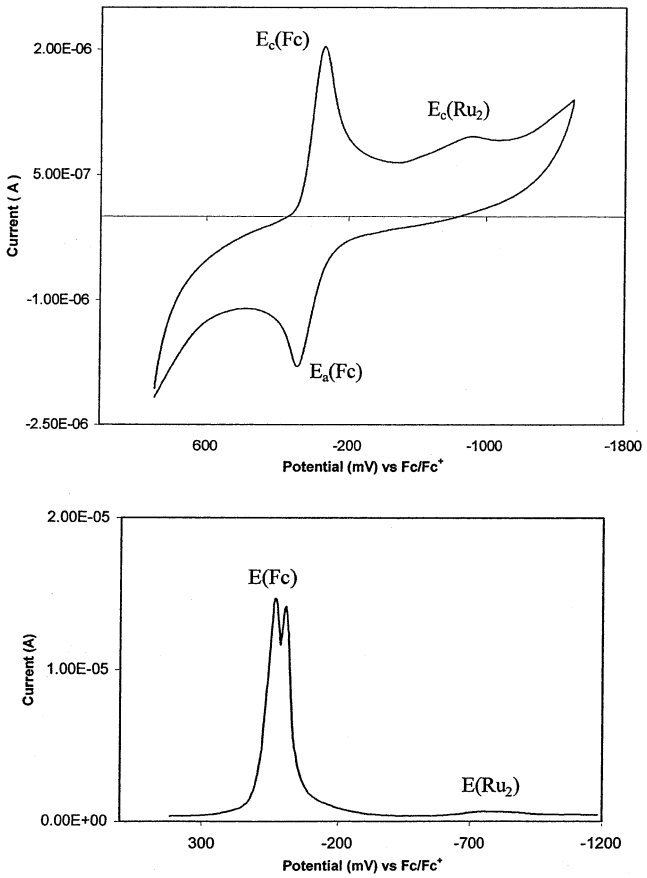

Figure 4. Top: Cyclic voltammogram of complex **10** in 1,2-dichloroethane (0.100 M TBAH) at a scan rate of 100 mV s^{-1} vs Fc^+/Fc (25 °C). Bottom: Osteryoung square-wave voltammogram of complex **10** under the same conditions as in above.

E(Fc) = −132 mV vs Fc^+/Fc (see left inset in Figure 3). The CV and OSWV behavior of complex **8** is very similar to that of **9** except with slightly more positive values of E_a(Fc) and E_c(Fc) (a trend already seen in the free acids). There was no observed diruthenium core reduction, which is most likely due to the more limited solubility of **8** in 1,2-dichloroethane. No peak splitting, as was seen for complex **7**, is seen for either **8** or **9** in the CV or the OSWV. Electrochemical data for all of the complexes are summarized in Table 5.

Complex **10** shows more interesting behavior. The CV and OSWV scans are shown in Figure 4. While the shape of the CV looks similar to that of complexes **8** and **9**, there are two differences. The reduction to oxidation current ratio (i_c/i_a = 1.6) at a scan rate of 100 mV s^{-1} is significantly less than that for complexes **7**−**9** (see Table 5). This is almost certainly due to the fact that the fully oxidized species of complex **10** is more soluble than the corresponding oxidized species for complexes **7**−**9**, and hence less deposition occurs at the electrode surface. It was also noted, qualitatively, that complex **10** itself was somewhat more soluble than complexes **7**−**9**. The second difference is that the bandwidths of both the oxidation and the reduction waves in **10** are slightly broader (about 20%) than the corresponding waves in the CVs of **8** and **9**. This led us to perform OSWV to see if we could resolve any peak splitting, and indeed Figure 4 (bottom) shows there to be a small but distinct separation (the OSWV measurements on **8** and **9** only showed single peaks). The peak-to-peak separation of 41 mV is less than that seen for complex **7** (75−90 mV) and close to the statistical limit (35.6 mV) for an uncoupled system. If through-bond coupling between iron centers is occurring, this would not be unexpected, as the shortest through-bond Fe−Fe distance in **10** is close to 6 Å longer (19.3 vs 13.5 Å) than in **7**. A through-space coupling mechanism seems unlikely, as the two closest intramolecular through-space Fe−Fe distances (those corresponding to the two sets of ferrocenyl groups facing each other, see Figure 1) are 7.3 Å for Fe(1)−Fe(4) and 7.6 Å for Fe(2)−Fe(3).

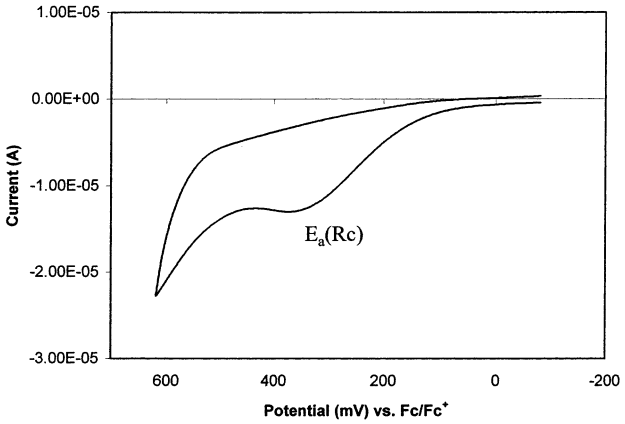

Figure 5. Cyclic voltammogram of complex **11** in DMF (0.100 M TBAH) showing the irreversible ruthenocenyl-centered oxidation (E_a(Rc)) at a scan rate of 100 mV s^{-1} vs Fc^+/Fc (25 °C).

Diruthenium Ruthenocenecarboxylate Derivative (11). As with the free acid, rcaH, complex **11** was not sufficiently soluble in a noncoordinating solvent to allow us to perform adequate electrochemical measurements, and so *N*,*N*′-dimethylformamide was chosen. The results, summarized in Table 5, are not unlike that of the free acid with an irreversible ruthenocenyl-centered oxidation wave (E_a(Rc)) in the CV at 374 mV vs Fc^+/Fc, in this case corresponding to eight electrons (from coulometry) (Figure 5). A very weak irreversible reduction wave (E_c) corresponding to the core $Ru_2^{5+/4+}$ reduction is also seen at −550 mV vs Fc^+/Fc in the CV. No evidence of any peak splitting is seen in the CV or OSWV.

It should be noted that the trends in the anodic and cathodic potentials for the metallocenyl-centered processes seem, in general, to parallel those of the free acids. The cathodic potentials of the diruthenium core show no discernible trend (either in the CV or in the OSWV).

Conclusion

The use of metallocene carboxylates as ligands offers a facile way to introduce additional metal centers around an existing metal center or centers. Using a simple carboxylate exchange reaction we have synthesized and fully characterized a series of diruthenium(II,III) tetrametallocenecarboxylato derivatives and structurally characterized the first known example of a transition metal complex containing ruthenocene carboxylate as a ligand. Structurally the $[Ru_2(rca)_4(1\text{-propanol})_2](PF_6)$ complex resembles the previously de-

termined $[Ru_2(fca)_4(1\text{-propanol})_2](PF_6)$ complex in that all four of the metallocenyl groups are pointing away from each other. In the $[Ru_2(fcpe)_4(1\text{-propanol})_2](PF_6)$ compound the addition of a −CH═CH− spacer between the carboxyl group and the Cp ring appears to allow the ferrocenyl groups more freedom of motion (less crowding), and they arrange themselves in two pairs facing each other.

Electrochemical measurements on these complexes showed a loss of the ferrocenyl−ferrocenyl communication seen in $[Ru_2(fca)_4(1\text{-propanol})_2](PF_6)$ when even one saturated spacer ($-CH_2-$ group) was introduced between the carboxyl moiety and the Cp ring. However, when a conjugated pathway is supplied (−CH═CH− spacer), a very small degree of interaction is still evident, as seen in the OSWV. A through-bond pathway for the coupling would seem most likely, as the through-space Fe−Fe distances are all greater than 7 Å. No interactions are seen for the ruthenocene carboxylate derivative, $[Ru_2(rca)_4(1\text{-propanol})_2](PF_6)$, as the electrochemistry reveals irreversible ruthenocene oxidation, reminiscent of the free acid. Current studies are directed toward the preparation of simpler, mononuclear ruthenium centers with one or more metallocene carboxylates attached (i.e., $L_xRu(\eta^2\text{-}O_2C(X)CpMCp)_y$, where L are spectator ligands, X is an appropriate spacer, and M = Fe or Ru) in order to further investigate the interactions in these unique systems.

Acknowledgment. M.A.S.A. thanks NSERC (Canada) for financial support.

Supporting Information Available: Two X-ray crystallographic files. This material is available free of charge via the Internet at http://pubs.acs.org.

OM020729B